Article

Cell Chemical Biology

Enhanced Cellular Polysulfides Negatively Regulate TLR4 Signaling and Mitigate Lethal Endotoxin Shock

Graphical Abstract

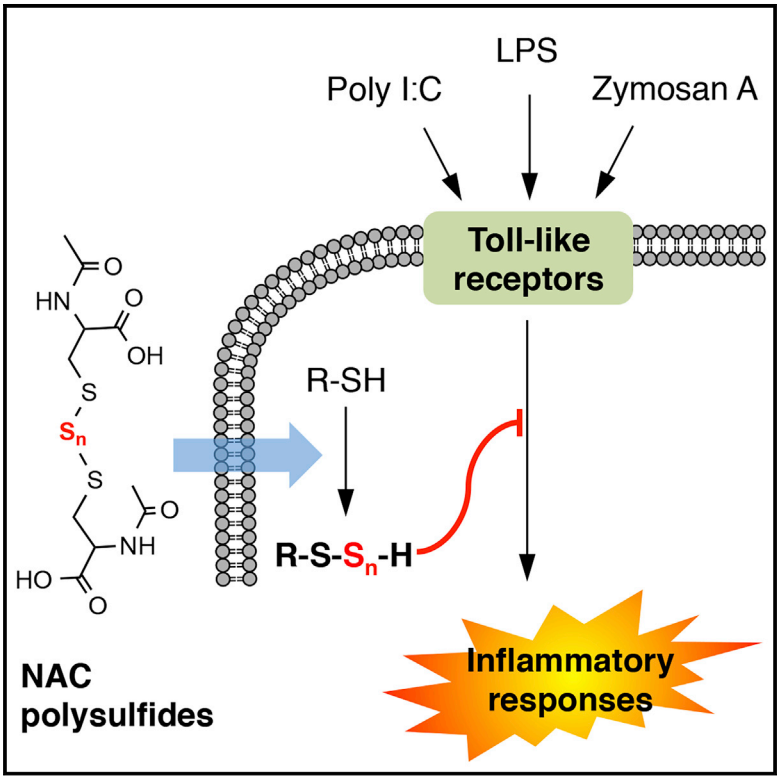

Authors

Tianli Zhang, Katsuhiko Ono, Hiroyasu Tsutsuki, Hideshi Ihara, Waliul Islam, Takaaki Akaike, Tomohiro Sawa

Correspondence

sawat@kumamoto-u.ac.jp

In Brief

Zhang et al. developed potent persulfide donors consisting of sulfane sulfur atoms stabilized by N-acetyl-L-cysteine (NAC polysulfides) via disulfide bonds at both sides. Strong anti-inflammatory activity of NAC polysulfides was demonstrated in cultured macrophage models and a mouse endotoxin shock model.

Highlights

- Cell-permeable, thiol-activable polysulfide donors are developed
- Polysulfide donor treatment increases intracellular polysulfide levels
- Polysulfide donor treatment desensitizes macrophages to TLRs signaling
- Mice are protected from lethal endotoxin shock by polysulfide donor treatment

Zhang et al., 2019, Cell Chemical Biology *26*, 1–13
May 16, 2019
https://doi.org/10.1016/j.chembiol.2019.02.003

CellPress

Please cite this article in press as: Zhang et al., Enhanced Cellular Polysulfides Negatively Regulate TLR4 Signaling and Mitigate Lethal Endotoxin Shock, Cell Chemical Biology (2019), https://doi.org/10.1016/j.chembiol.2019.02.003

Cell Chemical Biology
Article

Enhanced Cellular Polysulfides Negatively Regulate TLR4 Signaling and Mitigate Lethal Endotoxin Shock

Tianli Zhang,[1] Katsuhiko Ono,[1] Hiroyasu Tsutsuki,[1] Hideshi Ihara,[2] Waliul Islam,[1] Takaaki Akaike,[3] and Tomohiro Sawa[1,4,*]
[1]Department of Microbiology, Graduate School of Medical Sciences, Kumamoto University, Honjo 1-1-1, Chuo-ku, Kumamoto 860-8556, Japan
[2]Department of Biological Science, Graduate School of Science, Osaka Prefecture University, Osaka 599-8531, Japan
[3]Department of Environmental Medicine and Molecular Toxicology, Tohoku University Graduate School of Medicine, 2-1 Seiryo-machi, Aoba-ku, Sendai 980-8575, Japan
[4]Lead Contact
*Correspondence: sawat@kumamoto-u.ac.jp
https://doi.org/10.1016/j.chembiol.2019.02.003

SUMMARY

Cysteine persulfide and cysteine polysulfides are cysteine derivatives having sulfane sulfur atoms bound to cysteine thiol. Accumulating evidence has suggested that cysteine persulfides/polysulfides are abundant in prokaryotes and eukaryotes and play important roles in diverse biological processes such as antioxidant host defense and redox-dependent signal transduction. Here, we show that enhancement of cellular polysulfides by using polysulfide donors developed in this study resulted in marked inhibition of lipopolysaccharide (LPS)-initiated macrophage activation. Polysulfide donor treatment strongly suppressed LPS-induced pro-inflammatory responses in macrophages by inhibiting Toll-like receptor 4 (TLR4) signaling. Other TLR signaling stimulants—including zymosan A-TLR2 and poly(I:C)-TLR3—were also significantly suppressed by polysulfur donor treatment. Administration of polysulfide donors protected mice from lethal endotoxin shock. These data indicate that cellular polysulfides negatively regulate TLR4-mediated pro-inflammatory signaling and hence constitute a potential target for inflammatory disorders.

INTRODUCTION

Cysteine persulfide (CysSSH) and cysteine polysulfides ($CysS[S]_nH$, $n > 2$) are cysteine derivatives having sulfane sulfur atoms bound to cysteine thiol (Fukuto et al., 2018; Ida et al., 2014; Ono et al., 2014; Sawa et al., 2018). Accumulating evidence has suggested that cysteine persulfides/polysulfides are abundant in prokaryotes and eukaryotes in diverse forms such as monomeric amino acid hydropersulfides/polysulfides (CysSSH, $CysS[S]_nH$), reduced L-glutathione (GSH) hydropersulfides/polysulfides ($GS[S]_nH$), and protein persulfide/polysulfide residues (Akaike et al., 2017; Ida et al., 2014; Kunikata et al., 2017; Numakura et al., 2017; Ono et al., 2017; Peng et al., 2017). Hydropersulfides/polysulfides are highly potent antioxidants and hence protect cells from injury induced by reactive oxygen species (ROS) (Ida et al., 2014; Kunikata et al., 2017). $CysS[S]_nH$ were recently demonstrated to be critical components in mitochondrial sulfur respiration (Akaike et al., 2017). Also, hydropersulfide/polysulfide moieties occurring on protein thiols may be involved in redox-dependent regulation of protein functions (Millikin et al., 2016). We previously reported that the transsulfuration enzymes cystathionine β-synthase and cystathionine γ-lyase can produce CysSSH from cystine via C-S bond cleavage (Ida et al., 2014). Cysteinyl-tRNA synthetases (CARS) were recently found to act as potent CysSSH-producing enzymes by using cysteine as a substrate (Akaike et al., 2017). Furthermore, CARS can catalyze direct incorporation of CysSSH into proteins via *de novo* protein synthesis (Akaike et al., 2017).

Persulfide/polysulfide donors that can increase intracellular persulfide/polysulfide levels by donating their sulfur atoms to endogenous acceptor thiols become powerful chemical tools for understanding the physiological and pathological roles of persulfide species in biological systems. Powell et al. (2018) recently reported that N-acetyl-L-cysteine (NAC) conjugated to Bpin through disulfide bonding can act as a prodrug for a persulfide donor (BDP-NAC). BDP-NAC can release free NAC hydropersulfide (NAC-SH) in response to hydrogen peroxide exposure (Powell et al., 2018). Powell and colleagues also demonstrated that BDP-NAC treatment protected cells from cell death caused by hydrogen peroxide, possibly by producing antioxidant NAC-SH in cells (Powell et al., 2018). Their study, however, did not provide details of the metabolism of BDP-NAC and NAC-SH in cells, particularly the effects of BDP-NAC treatment on the intracellular persulfide/polysulfide metabolome. Zheng et al. (2017) developed a persulfide prodrug that generated a hydroxymethyl persulfide via esterase-dependent activation. They also reported that such a persulfide-generating prodrug exhibited potent cardioprotective effects in a murine model of myocardial ischemia-reperfusion injury with a bell-shaped therapeutic profile (Zheng et al., 2017). Kang et al. (2018) reported another class of persulfide precursors that produce hydropersulfides via pH- or F^--mediated desilylation of O-silyl mercaptan-based sulfur-containing molecules. Artaud and Galardon (2014) developed

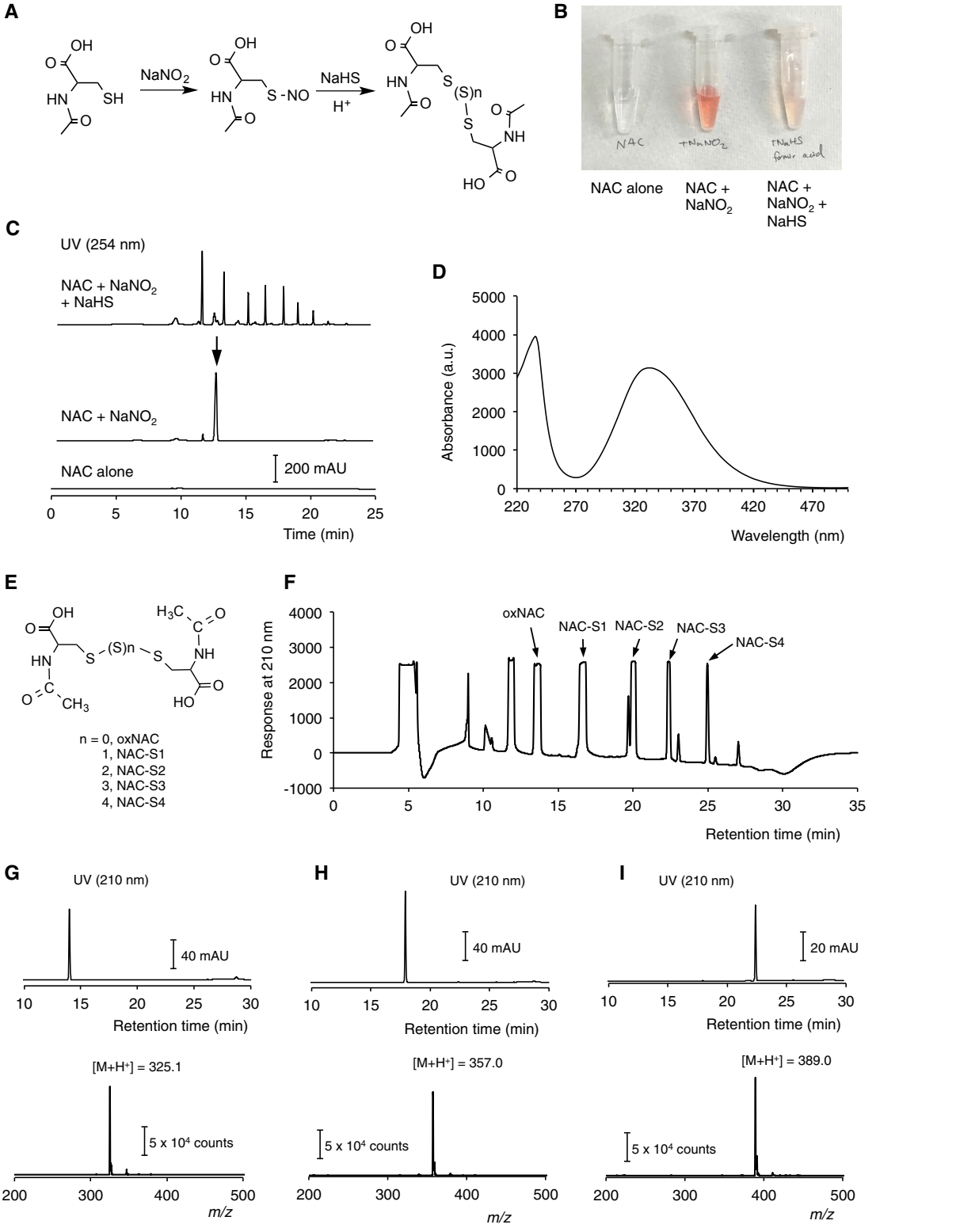

Figure 1. Synthesis and Purification of NAC Polysulfides

(A) Reaction scheme of the synthesis of NAC polysulfides.

(B) Appearance of the solutions of reduced NAC (left), reduced NAC reacted with $NaNO_2$ (center), and reduced NAC reacted with $NaNO_2$ and NaHS (right).

(C) HPLC chromatograms for reduced NAC (bottom), reduced NAC reacted with $NaNO_2$ (middle), and reduced NAC reacted with $NaNO_2$ and NaHS (top), detected at 254 nm.

(legend continued on next page)

disulfide precursors that spontaneously rearrange in neutral pH buffer to produce hydropersulfides. By using hydropersulfide-generating molecules, Fukuto and colleagues investigated the physicochemical and some biochemical properties of hydropersulfide species (Bianco et al., 2016; Millikin et al., 2016). We previously reported that $GS[S]_nH$ can be formed by glutathione reductase (GR)-mediated reduction of oxidized GSH polysulfides ($GS[S]_nSG$, $n > 1$) (Ida et al., 2014). Strong ROS-scavenging activity of $GS[S]_nH$ was demonstrated by using this $GS[S]_nSG$-GR system (Ida et al., 2014).

One unique characteristic of persulfides/polysulfides is that they can donate sulfane sulfur atoms to acceptor thiols via sulfur transfer reactions (Fukuto et al., 2018; Ono et al., 2014). Thus, related to this finding, we hypothesized that appropriate persulfides/polysulfides may act as persulfide/polysulfide donors in biological systems. In this study, we synthesized NAC polysulfides and examined their ability to act as persulfide/polysulfide donors *in vitro*, in cultured cells, and *in vivo*. We investigated sulfur transfer reactions between NAC polysulfides and acceptor thiols in detail by means of mass spectrometry (MS)-based sulfur metabolomic analysis. We studied the biological effects of NAC polysulfides on innate immune responses by using lipopolysaccharide (LPS)-activated cultured macrophages and a mouse endotoxin shock model. Our data showed that NAC polysulfides can act as potent persulfide/polysulfide donors in biological systems. In view of the strong anti-inflammatory activities of NAC polysulfides demonstrated in this study, persulfide/polysulfide donors may become therapeutic agents applicable for inflammation-associated diseases including sepsis.

RESULTS

Preparation of NAC Polysulfides

We successfully prepared NAC polysulfides having different numbers of sulfane sulfur atoms by reacting NAC with sodium nitrite ($NaNO_2$) and sodium hydrogen sulfide (NaHS) in aqueous media (Figure 1A). Formation of S-nitroso-NAC in the first step was suggested by the appearance of a characteristic reddish color and a high-performance liquid chromatography (HPLC) peak having a UV spectrum consistent with S-nitroso-NAC reported previously (Figures 1B–1D) (Shishido and de Oliveira, 2000). Addition of NaHS resulted in the disappearance of the S-nitroso-NAC peak and the appearance of several new peaks (Figure 1C). These new peaks were determined to be NAC polysulfides having different numbers of sulfane sulfur atoms by means of MS (Figures 1E–1I). NAC polysulfides were purified by means of reversed-phase chromatography on the basis of their different hydrophobicities (Figure 1F). After fractionation and lyophilization of the polysulfides, the purity of each NAC polysulfide was determined to be higher than 95% as determined by chromatograms at 210 nm (Figures 1G–1I). Although NAC-S3 and NAC-S4 were obtained as a single HPLC peak, lyophilized products showed mixtures of NAC polysulfides with various sulfur numbers, probably because of sulfur-sulfur bond rearrangements during lyophilization. Thus, we used NAC-S1 and NAC-S2 in the following experiments. We also used oxidized NAC (oxNAC) as a control reagent that lacks a sulfane sulfur atom.

NAC polysulfides were highly water soluble. For instance, oxNAC, NAC-S1, and NAC-S2 were freely soluble in neutral aqueous buffers at approximately up to 30 mM at room temperature.

Lyophilized NAC polysulfides were stable during storage in a freezer (−30°C) without detectable decomposition for more than 1 year. The stabilities of NAC polysulfides in physiological saline were also determined as a function of temperature and incubation periods. NAC polysulfides were stable during incubation at 37°C for 72 h in physiological saline (data not shown). After 12 days of incubation at 37°C, the concentration of NAC-S2 had decreased slightly to 85%, whereas oxNAC and NAC-S1 showed no detectable decrease (data not shown). At 5°C, no detectable loss of NAC polysulfides (oxNAC, NAC-S1, NAC-S2) occurred during up to 12 days of incubation (data not shown).

Sulfane Sulfur Transfer from NAC Polysulfides to Reduced GSH

To study sulfane sulfur transfer from NAC polysulfides to acceptor thiols, we investigated the reactions of NAC polysulfides with reduced thiols *in vitro* by using GSH as a biologically relevant thiol model. When 100 μM oxNAC was reacted with GSH (10 or 100 μM) in 100 mM sodium phosphate buffer (pH 7.4) at 37°C, oxNAC concentration showed no apparent change during an incubation period of up to 60 min (data not shown). In contrast, in the presence of GSH, concentrations of NAC-S1 and NAC-S2 decreased rapidly (Figures 2A and 2B). NAC-S1 decreased to 80% and 25% of the initial concentration at 30 min after incubation in the presence of 10 and 100 μM GSH, respectively (Figure 2A). The decrease in NAC-S2 in the presence of GSH occurred more quickly; only 20% and 5% of NAC-S2 remained in the presence of 10 and 100 μM GSH, respectively, after 30 min of incubation (Figure 2B).

Our MS-based assignment of the reaction products indicated the formation of various products in the reactions between NAC polysulfides and GSH (Figure S1). The reaction products found include NAC polysulfides with different sulfur numbers (oxNAC, NAC-S1, NAC-S2); mixed disulfides (GS-NAC), trisulfides (GS-S-NAC), and tetrasulfides (GS-SS-NAC) of GSH and NAC; reduced NAC and NAC hydropolysulfides (NAC-SH, NAC-SSH); GSH hydropersulfides/polysulfides (GSSH, GSSSH); and oxidized GSH (GSSG, GSSSG) in the reactions between NAC-S1 or NAC-S2 and GSH (Figures 2C, 2D, and S1). The occurrence of both reduced and oxidized forms of $GS[S]_nSG$ clearly suggests that NAC polysulfides can donate their sulfane sulfur atoms to the acceptor GSH via a sulfur transfer from an NAC polysulfide. We also detected hydrogen sulfide (H_2S), sulfite, and thiosulfate in the reactions between NAC polysulfides and GSH

(D) UV spectrum of the peak indicated by the arrow in (C).

(E) Structures of NAC polysulfides.

(F–I) Separation of the crude reaction mixture by using a C18 column (F). The reaction mixture (1.5 mL) consisting of NAC, $NaNO_2$, and NaHS was applied to a preparative C18 column. Peaks corresponding to NAC polysulfides were obtained and subjected to lyophilization. HPLC chromatograms (upper panel) and mass spectra (lower panels) of oxNAC (G), NAC-S1 (H), and NAC-S2 (I) after purification.

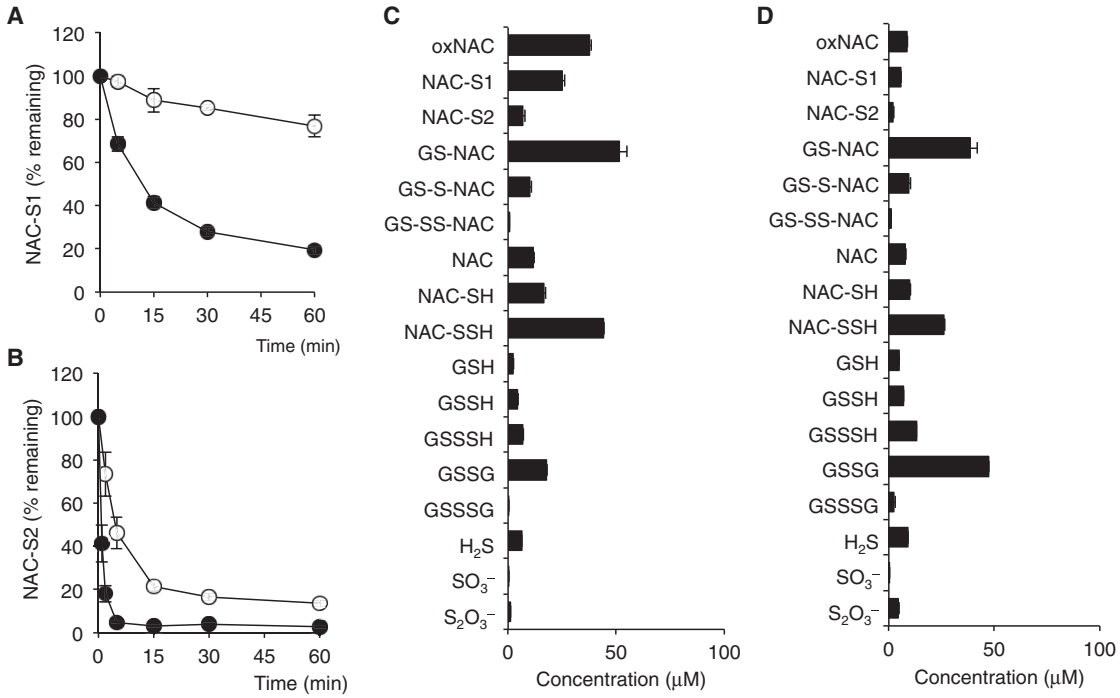

Figure 2. Reactions of NAC Polysulfides with GSH *In Vitro*

(A and B) Time-dependent alterations in NAC-S1 (A) and NAC-S2 (B) concentrations in the presence of GSH. NAC polysulfides (100 μM) were incubated in the presence of 10 μM GSH (open circles) or 100 μM GSH (closed circles) in 100 mM NaPB (pH 7.4) at 37°C for the indicated time periods. Residual amounts of NAC polysulfides were determined by means of LC-MS/MS.

(C and D) Product analyses for the reactions between NAC polysulfides and GSH. NAC-S1 (C) and NAC-S2 (D) at 100 μM were reacted with 100 μM GSH at 37°C for 30 min, followed by terminating the reactions by adding β-(4-hydroxyphenyl)ethyl acetamide (HPE-IAM). Reaction products were determined and quantified by means of LC-MS/MS. Data are means ± SD (n = 3).

(Figures 2C and 2D). These products may be derived from the reactions between hydropersulfides/polysulfides (e.g., NAC-SSH) and reduced thiols and subsequent auto-oxidation (Figure S2A). Figure S2A shows the possible reactions involved in the formation of such diverse products, with NAC-S2 used as an example. In these reactions, sulfane sulfur atoms in GSH persulfides/polysulfides likely derive from the sulfane sulfur atoms of NAC polysulfides. To confirm this expectation, we investigated the reaction of GSH with NAC-S2 labeled with the sulfur isotope ^{34}S at sulfane sulfur atoms (NAC-[^{34}S]2). Figure S2B clearly shows that GSSH and GSSSH formed in the reaction between NAC-[^{34}S]2 and GSH were labeled with ^{34}S.

Effects of NAC Polysulfide Treatment on the Intracellular Sulfur Metabolome

We then examined whether NAC polysulfides could be incorporated into cells and then act as sulfur donors to increase intracellular polysulfide levels. We used cells of the mouse macrophage-like cell line RAW264.7 because we wanted to clarify whether intracellular polysulfide levels affect the macrophage's responses to immunological stimuli. RAW264.7 cells were treated with NAC polysulfides in the absence (Figure S3A) or presence (Figure 3) of LPS. Intracellular sulfur species were quantified by means of liquid chromatography-tandem MS (LC-MS/MS). Figure 3A indicates that treatment of cells with oxNAC resulted in a marked increase in oxNAC in cells. Similarly, NAC-S1 treatment increased intracellular NAC-S1 levels (Figure 3B). These data suggest that NAC polysulfides were incorporated into cells when added to the culture medium. NAC-S2 treatment also increased intracellular NAC-S2 (Figure 3C), although the increase was quite small compared with that observed with oxNAC and NAC-S1 treatment (Figures 3A and 3B). This result may be due to the fact that incorporated NAC-S2 rapidly reacts with cellular thiols such as cysteine and GSH to donate its sulfane sulfur atoms, as observed in the *in vitro* experiments. This explanation is supported by the finding that NAC-S2 treatment markedly increased intracellular hydropersulfide/polysulfide levels of cysteine and GSH (Figures 3E, 3F, 3H, 3I, and 3L). We also found that NAC-S2 treatment significantly increased H_2S (Figure 3J) and thiosulfate (Figure 3Q) levels in cells. We detected mixed sulfides (GS-[S]$_n$-NAC; n = 0–2) in cells treated with NAC-S2 (Figures 3M–3O). However, those levels were very small compared with those of cysteine or GSH hydropersulfides/polysulfides. When cells were incubated with NAC-S2 for 6 h, cellular levels of hydropersulfides/polysulfides decreased (Figure S3B). Mechanisms or factors associated with this time-dependent decrease in intracellular polysulfide levels are currently not known and warrant further investigation. Similar responses to NAC polysulfide treatment were found for cells that did not receive LPS (Figure S3A). Reduced NAC, even at 5 mM, did not cause marked increases in intracellular polysulfide levels (Figure S3A). This result suggests

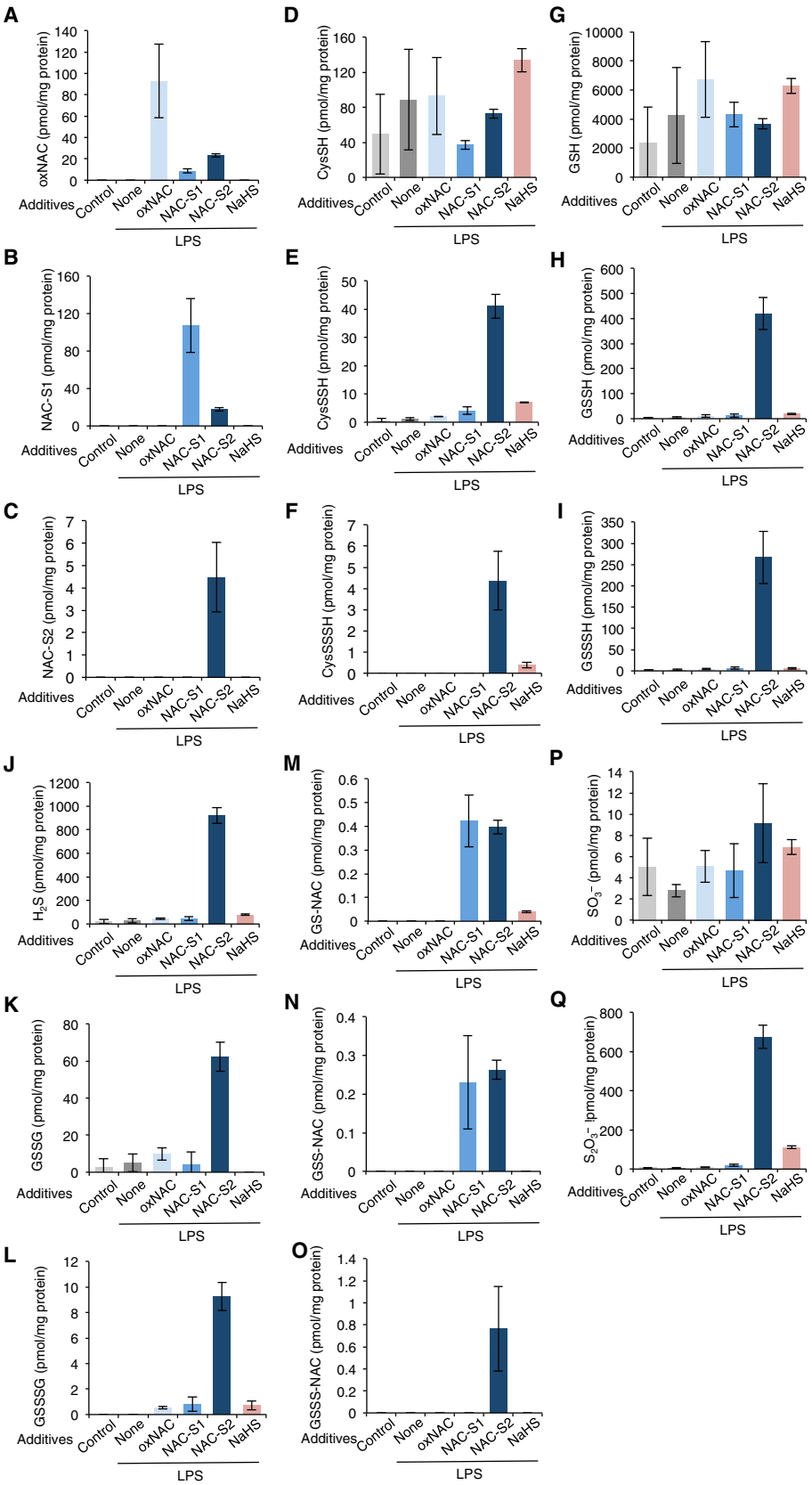

(legend on next page)

that NAC-S2 can act as a very effective sulfur donor in cell culture systems.

When cells were treated with NAC-S2 labeled with ^{34}S at sulfane sulfur atoms, intracellular hydropersulfides/polysulfides (e.g., GSSH and GSSSH), H_2S, and thiosulfate were labeled with ^{34}S (Figure S2C). This result indicates that the sulfur transfer from NAC-S2 to acceptor thiols is responsible for the increased persulfide/polysulfide levels in cells.

After 1 h of incubation, NAC-S1 treatment resulted in a small increase in hydropersulfides/polysulfides of cysteine and GSH as well as H_2S and thiosulfate (Figure 3). However, longer incubation periods (6 h) resulted in marked increases in polysulfide levels in cells treated with NAC-S1 (Figure S3B).

We also examined the effects of NaHS treatment on cellular polysulfide levels. We found that NaHS treatment increased levels of hydropersulfides/polysulfides of cysteine and GSH, but this effect was only marginal compared with that caused by NAC-S2 (Figures 3E, 3F, 3H, 3I, and 3L). In the case of NaHS treatment, no further increase in intracellular polysulfide levels was observed even after 6 h of incubation (Figure S3B). We expect that, collectively, NAC polysulfides, particularly NAC-S2, will be useful as efficient sulfur donors capable of increasing intracellular polysulfide levels and that this result may be achieved simply by adding the polysulfides to the culture media.

Suppression by NAC Polysulfide Treatment of Pro-inflammatory Responses in Macrophages Stimulated with LPS

As Figure 4A illustrates, RAW264.7 cells produced appreciable amounts of the pro-inflammatory cytokine tumor necrosis factor alpha (TNF-α) in response to LPS stimulation for 3 h. Statistically significant, marked inhibition of TNF-α production was found for cells after treatment with NAC-S2 (Figures 4A and S4A). Under the current experimental conditions, cell viability was not affected by NAC-S2 treatment (Figure 4B). These data indicate that pro-inflammatory responses of macrophages may be strongly suppressed by NAC-S2 treatment. TNF-α production by LPS-stimulated macrophages was not affected by oxNAC, NAC-S1, or NaHS under the present experimental conditions (Figure 4A). As Figures 4C and 4D show, LPS stimulation induced phosphorylation of IκBα and nuclear factor κB (NF-κB). We found that NAC-S2 treatment significantly inhibited phosphorylation of IκBα (Figures 4C and S4B) and NF-κB p65 (Figures 4D and S4C) in LPS-stimulated macrophages. LPS stimulation also induced a transient increase in the phosphorylation of extracellular signal-regulated kinase (ERK), p38 mitogen-activated protein (MAP) kinase, JNK, and Akt at 1 h after stimulation, after which those phosphorylation profiles returned to baseline levels (Figure 4E). We found that high phosphorylation levels of ERK, p38 MAP kinase, JNK, and Akt were maintained in cells treated with NAC-S2 (Figure 4E). Similar effects of NAC-S2 treatment on the phosphorylation of IκBα and ERK were found at early time points (Figures S4D–S4F). These data suggest that NAC-S2 treatment differently affected the phosphorylation network downstream of LPS-Toll-like receptor 4 (LPS-TLR4) signaling and that inhibition of the IκB kinase (IKK)/NF-κB axis may contribute to suppression of TNF-α production caused by NAC-S2 treatment (Scheme S1). Note that reduced NAC at concentrations up to 5 mM did not affect cytokine production by LPS-stimulated cells (Figures S5A and S5B). Under those conditions, no statistical increase in persulfides and polysulfides was found in LPS-stimulated RAW264.7 cells (Figures S5C–S5J).

LPS stimulation also induced production of another pro-inflammatory cytokine, interferon-β (IFN-β) (Figure 5). We found that LPS-induced IFN-β production was significantly inhibited by treatment not only with NAC-S2 but also with NAC-S1 (Figure 5A). After 6 h of incubation, cell viability was slightly but significantly reduced by NAC-S2 treatment (Figure 5B). Even if we consider this cell viability reduction, NAC-S2 treatment strongly suppressed IFN-β production by LPS-stimulated macrophages. IFN-β released extracellularly can then activate signal transducer and activator of transcription 1 (STAT1) signaling, which may lead to production of the inflammatory mediator nitric oxide (NO) via expression of inducible nitric oxide synthase (iNOS), in an autocrine and/or paracrine manner (Scheme S1). As Figures 5C–5F illustrate, all IFN-β downstream responses were markedly inhibited by NAC-S1 and NAC-S2. In our separate experiments, STAT1 phosphorylation induced by extracellularly added IFN-β was also strongly inhibited by NAC-S1 and NAC-S2 (Figure S6A). These data suggest that NAC polysulfides can suppress IFN-β-dependent inflammatory responses by inhibiting both IFN-β production and STAT1 phosphorylation. We also studied the effects of NAC polysulfides on the transcription of IFN-β by measuring IFN-β mRNA. As Figure S6B shows, NAC-S2 treatment reduced the level of IFN-β mRNA by approximately 50%, but NAC-S1 did not affect the transcription of IFN-β. This result suggests that NAC polysulfides may exert their inhibitory actions on IFN-β production during transcription and translation and that NAC-S2 can inhibit both processes.

We then examined whether NAC polysulfides affect signaling of other TLRs. RAW264.7 cells were stimulated with zymosan A and polyinosinic-polycytidylic acid (poly(I:C)) to activate TLR2 signaling (Young et al., 2001) and TLR3 signaling (Jiang et al., 2005), respectively. As Figure 6A shows, NAC-S2 treatment significantly reduced TNF-α production in cells stimulated with zymosan A and poly(I:C). These TLR ligands activated NF-κB phosphorylation that was suppressed by NAC-S2 treatment (Figures 6B and 6C).

Therapeutic Potential of NAC Polysulfides against Lethal Endotoxin Shock

Macrophage activation in response to LPS is an important innate immune response that helps eradication of Gram-negative bacteria. However, when host individuals are exposed to continuous LPS or large quantities of LPS, macrophages are overactivated

Figure 3. Metabolomic Determination of Intracellular Sulfur Species in RAW264.7 Cells Treated with NAC Polysulfides

Cells stimulated with LPS (100 ng/mL) were treated with 0.5 mM NAC polysulfides or NaHS for 1 h. Intracellular sulfur species were identified by means of LC-MS/MS as described in the STAR Methods. Controls were cells not treated with LPS or additives. Sulfur species analyzed were (A) oxNAC, (B) NAC-S1, (C) NAC-S2, (D) cysteine, (E) CysSSH, (F) CysSSSH, (G) GSH, (H) GSSH, (I) GSSSH, (J) H_2S, (K) GSSG, (L) GSSSG, (M) GS-NAC, (N) GSS-NAC, (O) GSSS-NAC, (P) sulfite, and (Q) thiosulfate. Data are means ± SD (n = 3).

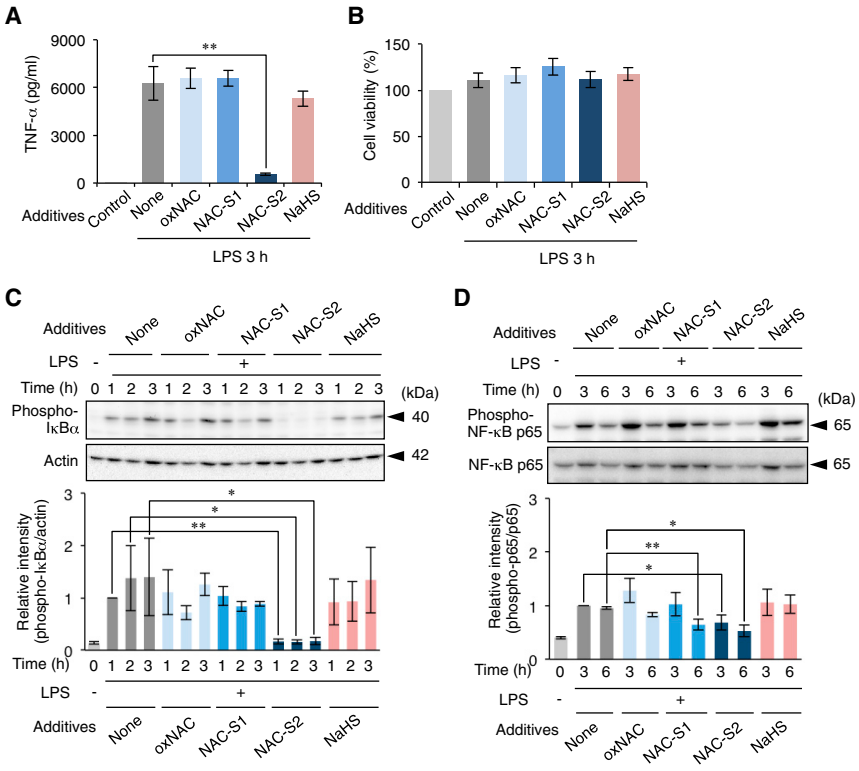

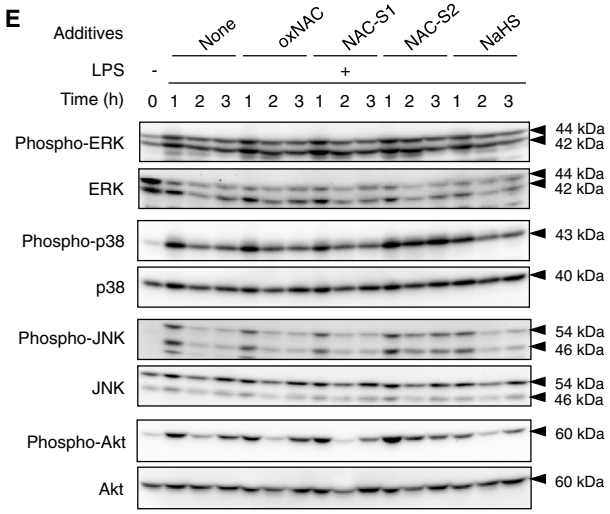

Figure 4. Effects of NAC Polysulfides on Innate Immune Responses of RAW264.7 Cells Stimulated by LPS

(A) Production of TNF-α from LPS-stimulated RAW264.7 cells and its suppression by NAC-S2. RAW264.7 cells were stimulated with LPS (100 ng/mL) for 3 h in the absence or presence of 0.5 mM NAC polysulfides or NaHS. TNF-α in culture supernatants was measured by means of ELISA.

(B–D) Cell viability (B) of RAW264.7 cells cultured under the same conditions as those for (A). Phosphorylation of IκBα (phospho-IκBα) (C) and of NF-κB p65 (phospho-NF-κB p65) (D) in RAW264.7 cells after LPS stimulation. Representative western blotting images (upper panels) and their quantitative data (lower panels). Controls were cells not treated with LPS or additives. Data are means ± SD (n = 3). *p < 0.05; **p < 0.01.

(E) Effects of NAC polysulfide treatments on the phosphorylation status of ERK, p38 MAP kinase, JNK, and Akt in RAW264.7 cells stimulated with LPS. At the indicated time points, lysates were prepared from RAW264.7 cells stimulated with 100 ng/mL LPS in the presence of 0.5 mM NAC polysulfides or NaHS. Representative western blotting images are shown.

to produce excess amounts of pro-inflammatory cytokines (a cytokine storm), which finally leads to lethal endotoxin shock (Cavaillon, 2018; Kuzmich et al., 2017). We used a mouse endotoxin shock model to see whether NAC polysulfides suppress LPS-induced macrophage activation *in vivo* and protect mice from lethal endotoxin shock. In the present experimental setting, 80% of mice died within 96 h after receiving intraperitoneal LPS (20 mg/kg body weight) (Figure 7A). Treatment with NAC polysulfides started 30 min after LPS administration. As Figure 7A shows, oxNAC treatment did not rescue mice from endotoxin shock. NAC-S1 treatment improved survival to 40%, but the effect did not reach statistical significance (Figure 7B). In the NAC-S2 treatment group, the survival rate was markedly improved; 90% of mice survived 96 h after LPS administration (p = 0.007 versus LPS + saline group, Figure 7C). This finding clearly suggested that NAC-S2 treatment effectively protected mice from lethal endotoxin shock *in vivo*. In sharp contrast, NaHS treatment failed to protect mice from endotoxin shock but rather significantly exacerbated the disorder (p = 0.0059 versus LPS + saline group, Figure 7D); all mice died within 48 h after treatment with NaHS (Figure 7D).

We then investigated cytokine production in this animal model. Serum samples obtained from mice given no LPS contained no detectable levels of TNF-α, but LPS administration induced a marked increase in serum TNF-α (Figure 7E). As an important finding, NAC-S2 treatment significantly reduced TNF-α levels in serum compared with the result obtained for the saline-treated group (Figure 7E). We also examined the production of INF-β in this animal model, but the serum levels were below the detection limit even after LPS administration (data not shown). As an interesting finding, NAC-S2 treatment significantly increased levels of persulfides, polysulfides, and thiosulfate in the lungs of mice compared with saline treatment (Figure S7A). This result suggests that NAC polysulfides can act as persulfide and polysulfide donors *in vivo*. Different responses to NAC-S2 treatment were observed in the liver (Figure S7B). Additional careful determination of the pharmacokinetics of NAC polysulfide administration to mice is ongoing. These data suggest that NAC polysulfides, particularly NAC-S2, can exert a protective

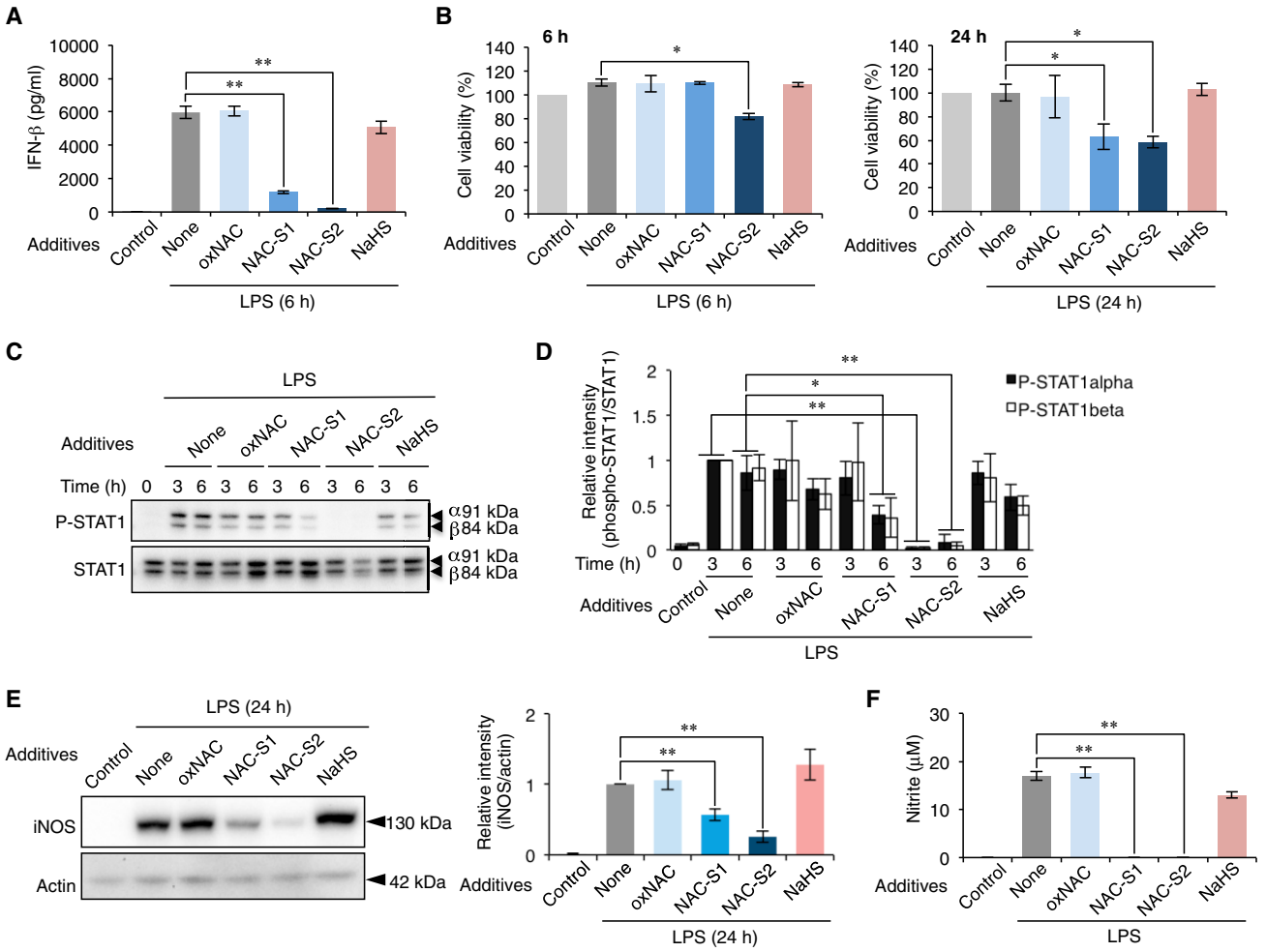

Figure 5. Suppression by NAC Polysulfides of IFN-β-Dependent Pro-inflammatory Responses in RAW264.7 Cells Stimulated with LPS

(A) Production of IFN-β from LPS-stimulated RAW264.7 cells and its suppression by NAC polysulfides. RAW264.7 cells were stimulated with LPS (100 ng/mL) for 6 h in the absence or presence of 0.5 mM NAC polysulfides or NaHS. IFN-β levels in culture supernatants were measured by means of ELISA.

(B) Viability of RAW264.7 cells cultured under various conditions for 6 h (left panel) and 24 h (right panel). Cells were treated with 100 ng/mL LPS in the presence of 0.5 mM NAC polysulfides or NaHS. Controls were cells not treated with LPS or additives. Data are means ± SD (n = 3).

(C) Western blotting of phosphorylation of STAT1 in RAW264.7 cells after LPS stimulation.

(D) Quantitative data for results in (C).

(E) Effects of NAC polysulfide treatment on iNOS expression by RAW264.7 cells stimulated with LPS. Expression of iNOS by cells 24 h after LPS stimulation was determined by means of western blotting. Representative western blotting image (left panel) and its quantitative data (right panel).

(F) Nitrite levels in culture supernatants of RAW264.7 cells. Nitrite levels were determined for culture supernatants obtained from RAW264.7 cells at 24 h after LPS stimulation by means of the Griess assay. Controls were cells not treated with LPS or additives.

Data are means ± SD (n = 3). *$p < 0.05$; **$p < 0.01$.

effect against lethal endotoxin shock by means of their anti-inflammatory functions, possibly through suppression of LPS-induced inflammatory responses.

DISCUSSION

In this study, we describe the preparation, physicochemical properties, sulfur-donating capabilities, and biological activities of NAC polysulfides. NAC polysulfides can easily be prepared by reacting NAC and sulfides in acidic media containing nitrite (Figure 1). NAC polysulfides may have certain advantages as persulfide/polysulfide donors. First, NAC polysulfides are stable during storage, even in aqueous media. This characteristic will save researchers the trouble of preparing fresh solutions just before each experiment. Second, one can easily prepare NAC polysulfides that are labeled with ^{34}S at sulfane sulfur moieties by using ^{34}S-sulfide as the starting material. Transfer of sulfur from ^{34}S-labeled NAC polysulfides and cellular acceptor thiols can thus be determined by monitoring isotope-labeled sulfur metabolomic data in complex biological milieu (e.g., Figure S2). Furthermore, researchers can study the metabolism of persulfides/polysulfides, with a particular focus on sulfane sulfur atoms, by detecting sulfur metabolites labeled with ^{34}S (Figure S2C). Third, decomposition metabolites that are derived

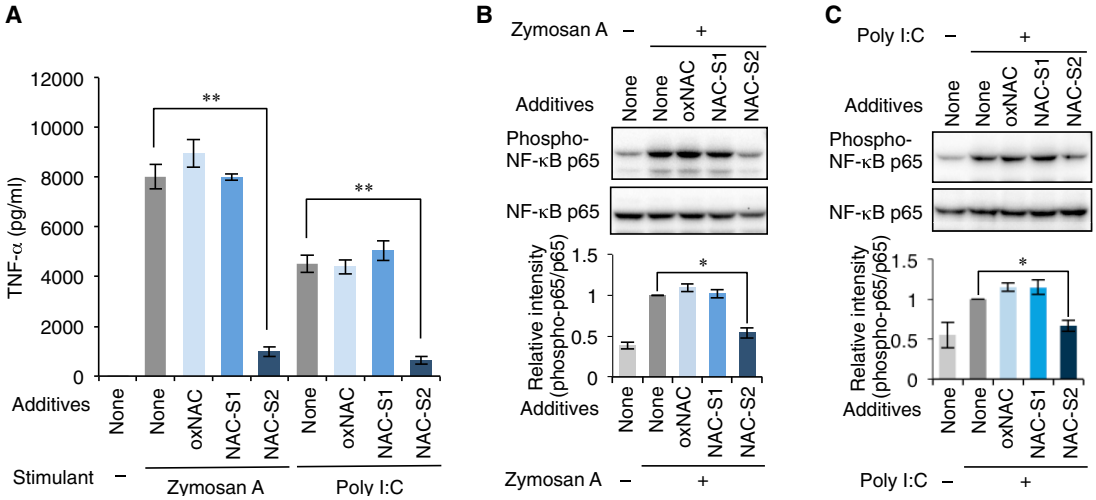

Figure 6. Effects of NAC-S2 on TLR2 and TLR3 Signaling in RAW264.7 Cells

RAW264.7 cells were stimulated with poly(I:C) (25 μg/mL) or zymosan A (100 μg/mL) for 3 h in the absence or presence of 0.5 mM NAC polysulfides. (A) Production of TNF-α from zymosan A- and poly(I:C)-stimulated RAW264.7 cells and its suppression by NAC-S2. TNF-α in culture supernatants was measured by means of ELISA. Phosphorylation of NF-κB p65 (phospho-NF-κB p65) in RAW264.7 cells treated with zymosan A (B) or poly(I:C) (C). Representative western blotting images (upper panels) and the related quantitative data (lower panels). Controls were cells not treated with ligands or additives. Data are means ± SD (n = 3). *$p < 0.05$; **$p < 0.01$.

from NAC polysulfides, including NAC itself, are expected to be biologically inert. Thus, one can expect that NAC polysulfides may be suitable for therapeutic purposes as prototype drugs if they have beneficial effects.

Our sulfur metabolomic analyses revealed that NAC polysulfides can donate their sulfane sulfur atoms to acceptor thiols such as GSH, which would result in the production of hydropersulfides/polysulfides *in vitro* and in cells (Figures 2, 3, and S1–S3). Reactions between NAC polysulfides and reduced thiols such as GSH can be initiated by a nucleophilic attack by reduced thiols, which would lead to formation of mixed sulfides and NAC hydropersulfides/polysulfides (NAC-SH, NAC-SSH), as expressed by Equations (1)–(3) in the case of NAC-S2 and GSH (Figure S2A).

$$GSH + NAC\text{-}SS\text{-}NAC \rightarrow GS\text{-}NAC + NAC\text{-}SSH \quad \text{(Equation 1)}$$

$$GSH + NAC\text{-}SS\text{-}NAC \rightarrow GS\text{-}S\text{-}NAC + NAC\text{-}SH \quad \text{(Equation 2)}$$

$$GSH + NAC\text{-}SS\text{-}NAC \rightarrow GS\text{-}SS\text{-}NAC + NAC \quad \text{(Equation 3)}$$

In fact, we detected all expected products derived according to Equations (1)–(3) (Figures 2 and S2A). The present data showed that the amounts of reaction products in Equation (1) (GS-NAC and NAC-SSH) were higher than those in Equation (2) and Equation (3) (GS-S-NAC and NAC-SH for Equation 2, GS-SS-NAC and NAC for Equation 3), which suggests that Equation (1) proceeded more favorably than did Equation (2) and Equation (3) (Figure 2D), probably because NAC-SSH behaves as a better leaving group than NAC-SH and NAC. GS-$[S]_n$-NAC (n = 1,2) formed in this way then reacts with reduced thiols to form GS$[S]_n$H, as expressed in Equation (4) (Figure S2A).

$$GS\text{-}[S]_n\text{-}NAC + NAC \rightarrow GS[S]_nH + RS\text{-}NAC \quad \text{(Equation 4)}$$
$$(n = 1,2)$$

The reaction between NAC-SSH and GSH, however, resulted in the formation of GSSSH (Equation 5, Figure S2A):

$$NAC\text{-}SSH + GSH \rightarrow NAC + GSSSH \quad \text{(Equation 5)}$$

Additional reactions between GS$[S]_n$H and reduced thiols produced HS_nH (Figure S2A). We detected appreciable amounts of thiosulfate in the reaction of NAC polysulfides and GSH, which suggests that H_2S_2 was oxidized under the current conditions to form thiosulfate (Figure S2A). We also detected GSSG in the reactions between NAC polysulfides and GSH (Figures 2C and 2D). GSSG can be formed according to Equation (6) and others.

$$GS[S]_nH + GSH \rightarrow H_2S_n + GSSG \quad \text{(Equation 6)}$$

In our cell culture experiments, we found similar reaction products in cells after NAC polysulfide treatment (Figure 3). This finding strongly supports the belief that NAC polysulfides can permeate cell membranes and donate their sulfane sulfurs to acceptor thiols such as cysteine and GSH that are present in cells, which would result in marked elevation of endogenous persulfide/polysulfide levels. We should note that, in cell experiments, we found appreciable amounts of sulfide (H_2S) and thiosulfate after NAC-S2 treatment for 1 h (Figure 3). This result suggests the existence in cells of metabolizing pathways for hydropersulfides/polysulfides to produce H_2S and thiosulfate. ETHE1, a mitochondrial-localized enzyme, can catalyze reductive degradation of GSSH to form GSH and sulfite with the use of molecular oxygen as a co-substrate (Jung et al., 2016; Kabil and Banerjee, 2012; Mineri et al., 2008). Sulfide:quinone oxidoreductase, also a mitochondrial enzyme, oxidizes sulfide to form sulfite, thiosulfate, or sulfate (Hildebrandt and Grieshaber, 2008). Thiosulfate is also formed in the reaction catalyzed by rhodanese with the use of sulfite and GSSH as substrates (Iciek et al., 2015). Organic hydropersulfides (RSSH)

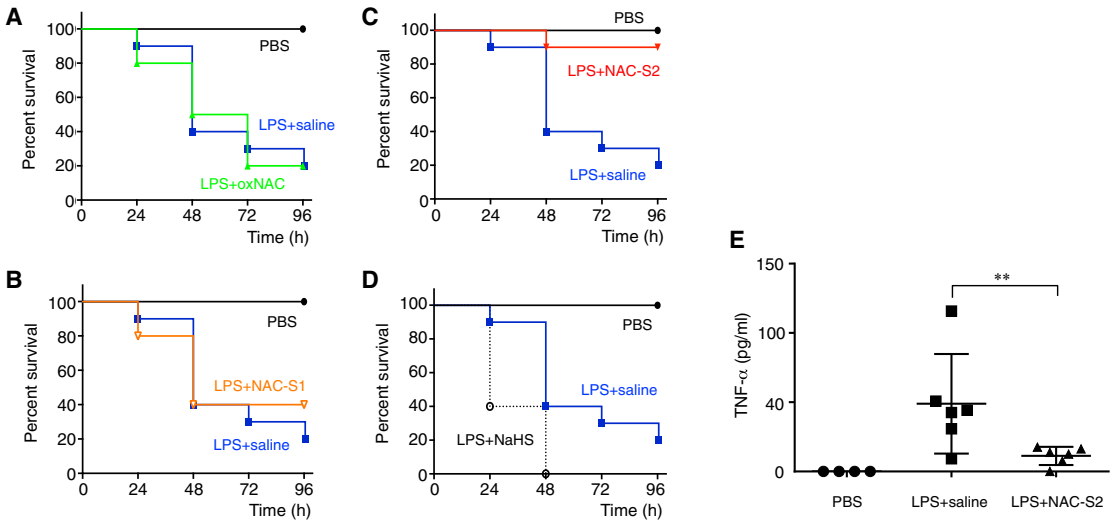

Figure 7. Protection of Mice from Lethal Endotoxin Shock by NAC-S2 Treatment

Mice received intraperitoneal LPS (20 mg/kg body weight) or PBS as a negative control. Thirty minutes after LPS administration, vehicle control (saline, A), oxNAC (A), NAC-S1 (B), NAC-S2 (C), or NaHS (D) (each at 120 μmol/kg) was injected intraperitoneally into mice. After 24 h, mice received the same treatment again. PBS control n = 6; each treatment group n = 10. In (E), serum TNF-α levels in mice receiving PBS alone (n = 4), LPS, and saline (n = 6), or LPS and NAC-S2 (n = 6) were measured. In the case of LPS and saline or NAC-S2 treatment, serum samples were collected 30 h after LPS administration. **$p < 0.01$.

can reportedly be enzymatically reduced to form corresponding thiols (RSH) and H_2S (Doka et al., 2016). In fact, Nagy and colleagues reported that thioredoxin reductase as well as GR may act as persulfide-reducing enzymes in cells to maintain persulfide homeostasis (Doka et al., 2016).

Ezerina et al. (2018) recently reported that treatment of adenocarcinoma cell lines with 10 mM reduced NAC resulted in the production of intracellular sulfane sulfur species as detected by using the sulfane sulfur probe SSip-1 DA. In the present study, we found that treatment of non-stimulated RAW264.7 cells with reduced NAC at 5 mM resulted in a marked increase in intracellular cysteine (Figure S3A), whereas we did not observe any increase in intracellular persulfides and polysulfides under these conditions, as determined by means of LC-MS/MS (Figures S3A and S5). This result suggests that the metabolism of reduced NAC may vary and depend on cell types, concentrations of reduced NAC, and incubation periods.

Innate immunity is the first line of defense against pathogenic invaders (Kawai and Akira, 2007, 2011; Kuzmich et al., 2017). The TLR family plays an important role in detecting various microbial components and in eliciting innate immunity (Kawai and Akira, 2007, 2011; Kuzmich et al., 2017). LPS, a cell wall component of Gram-negative bacteria, is recognized by TLR4 to activate expression of an array of inflammatory cytokine genes (Kawai and Akira, 2007, 2011; Kuzmich et al., 2017). TLR4-LPS signal transduction is initiated via the TIRAP-MyD88 and TRAM-TRIF pathways and leads to expression of inflammatory cytokines such as TNF-α and IFN-β, as illustrated in Scheme S1 (Kawai and Akira, 2007, 2011; Kuzmich et al., 2017). In this study, we found that NAC-S2 treatment strongly suppressed production of cytokines (TNF-α and IFN-β) from RAW264.7 cells stimulated with LPS (Figures 4, 5, S4, and S5). With regard to TNF-α production, signal pathways downstream of TIRAP-MyD88 include IKK and PI3K/AKT, which activate NK-κB, and MKK/MAPK, JNK, and ERK, which activate AP-1 (Scheme S1). Our western blotting analyses suggested that the IKK/NF-κB axis was markedly inhibited by NAC-S2 treatment (Figures 4 and S4), whereas the MKK/MAPK, JNK, and ERK pathways were instead activated by NAC-S2 treatment (Figure 4E). LPS-TLR4-NF-κB signaling was reportedly activated by ROS (Asehnoune et al., 2004). ROS may activate NF-κB signaling through IKK activation (Gloire et al., 2006) in a direct or an indirect manner via activation of upstream components of IKK activation such as PKD and SHIP-1 (Nakajima and Kitamura, 2013). As Figure 3 shows, NAC-S2 treatment rapidly increased levels of intracellular hydropersulfides/polysulfides, particularly GSSH and GSSSH to a significant extent. Because of the highly potent antioxidant properties of hydropersulfides/polysulfides, enhanced formation of these compounds by NAC-S2 treatment may result in reduced ROS levels in response to LPS stimulation. NAC-S2-mediated production of hydropersulfides/polysulfides may thus be a mechanism for reduced TNF-α production through the IKK/NF-κB axis. The TLR4 adaptor family MyD88 activates IRAK (IL-1R-associated kinase), which results in the recruitment of the protein kinase complex involving TAK1 (transforming growth factor-β-activated kinase-1) and TABs (TAK1-binding proteins) (Kawai and Akira, 2007). TAK1 has been suggested to activate two distinct pathways: the IKK-dependent NF-κB activation pathway and the MKK/MEK-dependent MAPK (ERK, JNK, p38) pathway (Kawai and Akira, 2007). As mentioned above, NAC-S2 treatment suppressed the NF-κB pathway and instead sustained ERK activation (Figure 4). Continued study is warranted to clarify the detailed molecular mechanisms involved in NAC-S2-mediated modulation of TLR4 signaling by identifying target molecules regulated by NAC-S2.

In addition to TLR4, TLR2, and TLR3 utilize TAK1 to activate NF-κB signaling, thereby leading to the production of pro-inflammatory cytokines including TNF-α (Kawai and Akira,

2007, 2011; Kuzmich et al., 2017). We found that NAC-S2 treatment strongly inhibited NF-κB activation and TNF-α production, induced by different TLR ligands such as zymosan A, poly(I:C), and LPS (Figures 4 and 6). Thus, the TAK1-NF-κB pathway may be a target for the anti-inflammatory actions of NAC-S2.

We found that IFN-β production was inhibited not only by NAC-S2 but also by NAC-S1 (Figure 5). Such reduced IFN-β production may be associated with NAC polysulfide-mediated inhibition of iNOS expression and NO production (Figure 5). IFN-β-induced phosphorylation of STAT1, which is essential for iNOS expression (Scheme S1), was also significantly inhibited by both NAC-S1 and NAC-S2 (Figure S6A). One hypothesis for why the TRAM-TRIF/IFN-β axis is inhibited by NAC-S1 is that TRAM-TRIF-mediated IFN-β production requires a longer activation period, such as 6 h, compared with that for the TIRAP-MyD88 pathway (Figure 5A). As seen in Figure S3B, a time-dependent increase in intracellular hydropersulfide/polysulfide levels was evident for cells treated with NAC-S1. Therefore, hydropersulfide/polysulfide levels may become sufficient to inhibit TRAM-TRIF pathways even in cells treated with NAC-S1.

NAC polysulfides may exert anti-inflammatory effects in addition to antioxidant actions. Protein thiols are expected to be modified by NAC polysulfides directly or via formation of low-molecular-weight hydropersulfides/polysulfides such as GSH hydropolysulfides. Inflammatory responses including NF-κB activation may be modulated through posttranslational thiol modifications such as protein sulfhydration (Paul and Snyder, 2012). Stimulator of interferon genes (STING) is one of the innate immune adaptor proteins essential for infection-induced production of type I IFNs (Ishikawa et al., 2009). S-Palmitoylation of cysteine at 91 (Cys91) of STING is critical for STING clustering and activation (Mukai et al., 2016). Haag et al. (2018) recently discovered that nitrofuran-type small molecules inhibited S-palmitoylation-induced STING activation through covalent binding to Cys91 of STING. This finding suggests that NAC polysulfides may exert their inhibitory actions on IFN-β production by modulating STING activity in a protein S-sulfhydration-dependent manner. Several S-sulfhydration proteomics methods have been developed, including a modified biotin-switch assay (Pan and Carroll, 2013), tag-switch assay (Ida et al., 2014; Zhang et al., 2014), protein persulfide detection protocol (Doka et al., 2016), and polyethylene glycol-conjugated maleimide-labeling gel shift assay (Akaike et al., 2017); these techniques may become powerful tools to identify target proteins as well as signaling cascades affected by protein S-sulfhydration. Additional study is thus warranted to determine the effects of NAC polysulfide treatment on the S-sulfhydration proteome, and particularly its association with LPS-TLR signaling cascade activity.

Although activation of TLR4 signaling is an important response for eradicating pathogenic invaders, excessive and dysregulated activation of TLR4 signaling related to LPS overload leads to endotoxin shock, which results in acute, life-threatening organ dysfunctions (Cavaillon, 2018; Kuzmich et al., 2017). Endotoxin shock, with increased LPS levels in blood, overexpression of pro-inflammatory cytokines, activation of the blood coagulation system, and accumulation of fibrinogen dysfunction products, causes a breakdown of local and general hemodynamics and endothelial dysfunction via TLR signaling pathways (Kuzmich et al., 2017). Various compounds have been tested in animal models for their ability to block TLR4-mediated cytokine production, and several have been tested in clinical trials (Kuzmich et al., 2017). The known TLR4 antagonists belong to different classes of chemical compounds, primarily glycolipids, which mimic the natural TLR4 ligand lipid A, but also heterocyclic compounds, peptides, opioids, steroids, taxanes, and others, and these compounds have natural and synthetic origins (Kuzmich et al., 2017).

In this study, we demonstrated that NAC-S2 treatment protected mice from lethal endotoxin shock, with a concomitant reduction in TNF-α production (Figure 7). This result suggests that persulfide/polysulfide donors may be applicable as TLR4 antagonists that can be used to treat endotoxin shock. Persulfide/polysulfide donors solely or in combination with other TLR4 antagonists warrant additional investigation as potential therapeutic agents.

In summary, we demonstrated here that NAC polysulfides are cell permeable and are reduced thiol-activable persulfide/polysulfide donors. NAC polysulfides strongly desensitize macrophages to TLR-mediated innate immune responses that accompanies reduced production of pro-inflammatory cytokines. NAC polysulfides may thus become powerful chemical tools for studying biological processes that are sensitive to endogenous persulfide/polysulfide levels and for developing strategies to treat pathological conditions associated with dysregulated inflammatory responses. Integrated omics approaches combining genomic, transcriptomic, proteomic, and metabolomic analyses may help understanding of the mechanisms of how NAC polysulfides modulate cellular responses by influencing thousands of cell signaling processes.

SIGNIFICANCE

Chemical compounds that effectively eliminate (scavengers) or enhance (donors) endogenous persulfides and polysulfides may become powerful tools for studying the biological roles of reactive sulfur species. This work reports that sulfane sulfur atoms stabilized by NAC (NAC polysulfides) via disulfide bonds at both sides can act as potent persulfide and polysulfide donors in cells. Mechanistic studies revealed that sulfane sulfur atoms in NAC polysulfides are readily transferred to acceptor thiols present in cells. The major findings of this study are that innate immune responses in macrophages that are governed by TLR signaling are highly affected by endogenous persulfide/polysulfide levels and that they are strongly suppressed by NAC polysulfides. In addition, NAC polysulfides had anti-inflammatory functions in mice and thus protected mice from lethal endotoxin shock. NAC polysulfides developed in this study will be useful to investigators who are interested in studying the roles of reactive sulfur species, including regulatory roles of these species in immune responses.

STAR★METHODS

Detailed methods are provided in the online version of this paper and include the following:

- KEY RESOURCES TABLE
- CONTACT FOR REAGENT AND RESOURCE SHARING

SUPPLEMENTAL INFORMATION

Supplemental Information includes seven figures, one table, and one scheme and can be found with this article online at https://doi.org/10.1016/j.chembiol.2019.02.003.

ACKNOWLEDGMENTS

We thank J.B. Gandy for her editing of the manuscript. This work was supported in part by Grants-in-Aid for Scientific Research ([A], [B], [C], Innovative Areas [Research in a Proposed Area], and Challenging Exploratory Research) from the Ministry of Education, Science, Sports, and Technology (MEXT), Japan, to H.T. (17K10019), H.I. (16H04674 and 26111011), T.A. (26111008, 26111001, and 16K15208), and T.S. (17K19205 and 18H02098); a grant from the Japan Agency for Medical Research and Development (AMED) to T.S. (JP18fm0208029); a grant from the Smoking Research Foundation to H.I.; a grant from the Takeda Science Foundation to K.O. and H.T.; and a grant from the Otsuka Toshimi Scholarship Foundation to T.Z.

AUTHOR CONTRIBUTIONS

T.S. designed the study. T.Z., K.O., H.T., H.I., W.I., and T.A. conducted the experiments. T.Z., K.O., and H.T. analyzed the data. T.S. and T.Z. wrote the manuscript. T.S. and T.A. edited the manuscript.

DECLARATION OF INTERESTS

The authors declare no competing interests.

Received: September 12, 2018
Revised: December 3, 2018
Accepted: January 31, 2019
Published: March 7, 2019

REFERENCES

Akaike, T., Ida, T., Wei, F.Y., Nishida, M., Kumagai, Y., Alam, M.M., Ihara, H., Sawa, T., Matsunaga, T., Kasamatsu, S., et al. (2017). Cysteinyl-tRNA synthetase governs cysteine polysulfidation and mitochondrial bioenergetics. Nat. Commun. *8*, 1177.

Artaud, I., and Galardon, E. (2014). A persulfide analogue of the nitrosothiol SNAP: formation, characterization and reactivity. Chembiochem *15*, 2361–2364.

Asehnoune, K., Strassheim, D., Mitra, S., Kim, J.Y., and Abraham, E. (2004). Involvement of reactive oxygen species in Toll-like receptor 4-dependent activation of NF-κ B. J. Immunol. *172*, 2522–2529.

Bianco, C.L., Chavez, T.A., Sosa, V., Saund, S.S., Nguyen, Q.N.N., Tantillo, D.J., Ichimura, A.S., Toscano, J.P., and Fukuto, J.M. (2016). The chemical biology of the persulfide (RSSH)/perthiyl (RSS) redox couple and possible role in biological redox signaling. Free Radic. Biol. Med. *101*, 20–31.

Cavaillon, J.M. (2018). Exotoxins and endotoxins: inducers of inflammatory cytokines. Toxicon *149*, 45–53.

Doka, E., Pader, I., Biro, A., Johansson, K., Cheng, Q., Ballago, K., Prigge, J.R., Pastor-Flores, D., Dick, T.P., Schmidt, E.E., et al. (2016). A novel persulfide detection method reveals protein persulfide- and polysulfide-reducing functions of thioredoxin and glutathione systems. Sci. Adv. *2*, e1500968.

Ezerina, D., Takano, Y., Hanaoka, K., Urano, Y., and Dick, T.P. (2018). N-Acetyl cysteine functions as a fast-acting antioxidant by triggering intracellular H_2S and sulfane sulfur production. Cell Chem. Biol. *25*, 447–459.

Fukuto, J.M., Ignarro, L.J., Nagy, P., Wink, D.A., Kevil, C.G., Feelisch, M., Cortese-Krott, M.M., Bianco, C.L., Kumagai, Y., Hobbs, A.J., et al. (2018). Biological hydropersulfides and related polysulfides - a new concept and perspective in redox biology. FEBS Lett. *592*, 2140–2152.

Furukawa, T., Yahiro, K., Tsuji, A.B., Terasaki, Y., Morinaga, N., Miyazaki, M., Fukuda, Y., Saga, T., Moss, J., and Noda, M. (2011). Fatal hemorrhage induced by subtilase cytotoxin from Shiga-toxigenic *Escherichia coli*. Microb. Pathog. *50*, 159–167.

Gloire, G., Legrand-Poels, S., and Piette, J. (2006). NF-κB activation by reactive oxygen species: fifteen years later. Biochem. Pharmacol. *72*, 1493–1505.

Haag, S.M., Gulen, M.F., Reymond, L., Gibelin, A., Abrami, L., Decout, A., Heymann, M., van der Goot, F.G., Turcatti, G., Behrendt, R., et al. (2018). Targeting STING with covalent small-molecule inhibitors. Nature *559*, 269–273.

Hildebrandt, T.M., and Grieshaber, M.K. (2008). Three enzymatic activities catalyze the oxidation of sulfide to thiosulfate in mammalian and invertebrate mitochondria. FEBS J. *275*, 3352–3361.

Iciek, M., Kowalczyk-Pachel, D., Bilska-Wilkosz, A., Kwiecien, I., Gorny, M., and Wlodek, L. (2015). S-Sulfhydration as a cellular redox regulation. Biosci. Rep. *36*, e00304.

Ida, T., Sawa, T., Ihara, H., Tsuchiya, Y., Watanabe, Y., Kumagai, Y., Suematsu, M., Motohashi, H., Fujii, S., Matsunaga, T., et al. (2014). Reactive cysteine persulfides and *S*-polythiolation regulate oxidative stress and redox signaling. Proc. Natl. Acad. Sci. U S A *111*, 7606–7611.

Ishikawa, H., Ma, Z., and Barber, G.N. (2009). STING regulates intracellular DNA-mediated, type I interferon-dependent innate immunity. Nature *461*, 788–792.

Jiang, W., Sun, R., Wei, H., and Tian, Z. (2005). Toll-like receptor 3 ligand attenuates LPS-induced liver injury by down-regulation of toll-like receptor 4 expression on macrophages. Proc. Natl. Acad. Sci. U S A *102*, 17077–17082.

Jung, M., Kasamatsu, S., Matsunaga, T., Akashi, S., Ono, K., Nishimura, A., Morita, M., Abdul Hamid, H., Fujii, S., Kitamura, H., et al. (2016). Protein polysulfidation-dependent persulfide dioxygenase activity of ethylmalonic encephalopathy protein 1. Biochem. Biophys. Res. Commun. *480*, 180–186.

Kabil, O., and Banerjee, R. (2012). Characterization of patient mutations in human persulfide dioxygenase (ETHE1) involved in H_2S catabolism. J. Biol. Chem. *287*, 44561–44567.

Kang, J., Xu, S., Radford, M.N., Zhang, W., Kelly, S.S., Day, J.J., and Xian, M. (2018). O→S relay deprotection: a general approach to controllable donors of reactive sulfur species. Angew. Chem. Int. Ed. *57*, 5893–5897.

Kawai, T., Adachi, O., Ogawa, T., Takeda, K., and Akira, S. (1999). Unresponsiveness of MyD88-deficient mice to endotoxin. Immunity *11*, 115–122.

Kawai, T., and Akira, S. (2007). Signaling to NF-κB by toll-like receptors. Trends Mol. Med. *13*, 460–469.

Kawai, T., and Akira, S. (2011). Regulation of innate immune signalling pathways by the tripartite motif (TRIM) family proteins. EMBO Mol. Med. *3*, 513–527.

Kunikata, H., Ida, T., Sato, K., Aizawa, N., Sawa, T., Tawarayama, H., Murayama, N., Fujii, S., Akaike, T., and Nakazawa, T. (2017). Metabolomic

profiling of reactive persulfides and polysulfides in the aqueous and vitreous humors. Sci. Rep. *7*, 41984.

Kuzmich, N.N., Sivak, K.V., Chubarev, V.N., Porozov, Y.B., Savateeva-Lyubimova, T.N., and Peri, F. (2017). TLR4 signaling pathway modulators as potential therapeutics in inflammation and sepsis. Vaccines *5*, https://doi.org/10.3390/vaccines5040034.

Marzinzig, M., Nussler, A.K., Stadler, J., Marzinzig, E., Barthlen, W., Nussler, N.C., Beger, H.G., Morris, S.M., Jr., and Bruckner, U.B. (1997). Improved methods to measure end products of nitric oxide in biological fluids: nitrite, nitrate, and *S*-nitrosothiols. Nitric Oxide *1*, 177–189.

Millikin, R., Bianco, C.L., White, C., Saund, S.S., Henriquez, S., Sosa, V., Akaike, T., Kumagai, Y., Soeda, S., Toscano, J.P., et al. (2016). The chemical biology of protein hydropersulfides: studies of a possible protective function of biological hydropersulfide generation. Free Radic. Biol. Med. *97*, 136–147.

Mineri, R., Rimoldi, M., Burlina, A.B., Koskull, S., Perletti, C., Heese, B., von Dobeln, U., Mereghetti, P., Di Meo, I., Invernizzi, F., et al. (2008). Identification of new mutations in the *ETHE1* gene in a cohort of 14 patients presenting with ethylmalonic encephalopathy. J. Med. Genet. *45*, 473–478.

Mukai, K., Konno, H., Akiba, T., Uemura, T., Waguri, S., Kobayashi, T., Barber, G.N., Arai, H., and Taguchi, T. (2016). Activation of STING requires palmitoylation at the Golgi. Nat. Commun. *7*, 11932.

Nakajima, S., and Kitamura, M. (2013). Bidirectional regulation of NF-κB by reactive oxygen species: a role of unfolded protein response. Free Radic. Biol. Med. *65*, 162–174.

Nakamura, Y., Kitagawa, T., Ihara, H., Kozaki, S., Moriyama, M., and Kannan, Y. (2006). Potentiation by high potassium of lipopolysaccharide-induced nitric oxide production from cultured astrocytes. Neurochem. Int. *48*, 43–49.

Numakura, T., Sugiura, H., Akaike, T., Ida, T., Fujii, S., Koarai, A., Yamada, M., Onodera, K., Hashimoto, Y., Tanaka, R., et al. (2017). Production of reactive persulfide species in chronic obstructive pulmonary disease. Thorax *72*, 1074–1083.

Ono, K., Akaike, T., Sawa, T., Kumagai, Y., Wink, D.A., Tantillo, D.J., Hobbs, A.J., Nagy, P., Xian, M., Lin, J., et al. (2014). Redox chemistry and chemical biology of H_2S, hydropersulfides, and derived species: implications of their possible biological activity and utility. Free Radic. Biol. Med. *77*, 82–94.

Ono, K., Jung, M., Zhang, T., Tsutsuki, H., Sezaki, H., Ihara, H., Wei, F.Y., Tomizawa, K., Akaike, T., and Sawa, T. (2017). Synthesis of l-cysteine derivatives containing stable sulfur isotopes and application of this synthesis to reactive sulfur metabolome. Free Radic. Biol. Med. *106*, 69–79.

Pan, J., and Carroll, K.S. (2013). Persulfide reactivity in the detection of protein *S*-sulfhydration. ACS Chem. Biol. *8*, 1110–1116.

Paul, B.D., and Snyder, S.H. (2012). H_2S signalling through protein sulfhydration and beyond. Nat. Rev. Mol. Cell Biol. *13*, 499–507.

Peng, H., Shen, J., Edmonds, K.A., Luebke, J.L., Hickey, A.K., Palmer, L.D., Chang, F.J., Bruce, K.A., Kehl-Fie, T.E., Skaar, E.P., et al. (2017). Sulfide homeostasis and nitroxyl intersect via formation of reactive sulfur species in *Staphylococcus aureus*. mSphere *2*, https://doi.org/10.1128/mSphere.00082-17.

Powell, C.R., Dillon, K.M., Wang, Y., Carrazzone, R.J., and Matson, J.B. (2018). A persulfide donor responsive to reactive oxygen species: insights into reactivity and therapeutic potential. Angew. Chem. Int. Ed. *57*, 6324–6328.

Sawa, T., Ono, K., Tsutsuki, H., Zhang, T., Ida, T., Nishida, M., and Akaike, T. (2018). Reactive cysteine persulphides: occurrence, biosynthesis, antioxidant activity, methodologies, and bacterial persulphide signalling. Adv. Microb. Physiol. *72*, 1–28.

Shishido, S.M., and de Oliveira, M.G. (2000). Polyethylene glycol matrix reduces the rates of photochemical and thermal release of nitric oxide from *S*-nitroso-*N*-acetylcysteine. Photochem. Photobiol. *71*, 273–280.

Sugiyama, T., Fujita, M., Koide, N., Mori, I., Yoshida, T., Mori, H., and Yokochi, T. (2004). 2-Aminopurine inhibits lipopolysaccharide-induced nitric oxide production by preventing IFN-β production. Microbiol. Immunol. *48*, 957–963.

Wintner, E.A., Deckwerth, T.L., Langston, W., Bengtsson, A., Leviten, D., Hill, P., Insko, M.A., Dumpit, R., VandenEkart, E., Toombs, C.F., et al. (2010). A monobromobimane-based assay to measure the pharmacokinetic profile of reactive sulphide species in blood. Br. J. Pharmacol. *160*, 941–957.

Young, S.H., Ye, J., Frazer, D.G., Shi, X., and Castranova, V. (2001). Molecular mechanism of tumor necrosis factor-α production in →3-β-glucan (zymosan)-activated macrophages. J. Biol. Chem. *276*, 20781–20787.

Zhang, D., Macinkovic, I., Devarie-Baez, N.O., Pan, J., Park, C.M., Carroll, K.S., Filipovic, M.R., and Xian, M. (2014). Detection of protein *S*-sulfhydration by a tag-switch technique. Angew. Chem. Int. Ed. *53*, 575–581.

Zheng, Y., Yu, B., Li, Z., Yuan, Z., Organ, C.L., Trivedi, R.K., Wang, S., Lefer, D.J., and Wang, B. (2017). An esterase-sensitive prodrug approach for controllable delivery of persulfide species. Angew. Chem. Int. Ed. *56*, 11749–11753.

Please cite this article in press as: Zhang et al., Enhanced Cellular Polysulfides Negatively Regulate TLR4 Signaling and Mitigate Lethal Endotoxin Shock, Cell Chemical Biology (2019), https://doi.org/10.1016/j.chembiol.2019.02.003

STAR★METHODS

KEY RESOURCES TABLE

REAGENT or RESOURCE	SOURCE	IDENTIFIER
Antibodies		
Rabbit polyclonal anti-actin antibody	Sigma-Aldrich	Cat#A2066; RRID: AB_476693
Mouse monoclonal anti-phospho-IκBα	Cell Signaling Technology	Cat#9246; RRID: AB_2267145
Rabbit monoclonal anti-phospho-STAT1	Cell Signaling Technology	Cat#7649; RRID: AB_11220426
Rabbit polyclonal anti-STAT1	Cell Signaling Technology	Cat#9172; RRID: AB_10693929
Rabbit monoclonal anti-phospho-NF-κB p65	Cell Signaling Technology	Cat#3033; RRID: AB_331284
Rabbit monoclonal anti-phospho-p44/42 MAPK(ERK1/2)	Cell Signaling Technology	Cat#4370; RRID: AB_2315112
Rabbit monoclonal anti- p44/42 MAPK(ERK1/2)	Cell Signaling Technology	Cat#4695; RRID: AB_390779
Rabbit monoclonal anti-phospho-SAPK/JNK	Cell Signaling Technology	Cat#4668; RRID: AB_2307320
Rabbit polyclonal anti-SAPK/JNK	Cell Signaling Technology	Cat#9252; RRID: AB_2250373
Rabbit monoclonal anti-phospho-Akt	Cell Signaling Technology	Cat#4060; RRID: AB_2315049
Rabbit monoclonal anti-Akt	Cell Signaling Technology	Cat#4691; RRID: AB_915783
Rabbit monoclonal anti-phospho-p38	Cell Signaling Technology	Cat#4511; RRID: AB_2139682
Rabbit monoclonal anti-p38	Cell Signaling Technology	Cat#8690; RRID: AB_10999090
Rabbit polyclonal anti-NF-κB p65 antibody	Santa Cruz Biotechnology	Cat#sc-372; RRID: AB_632037
iNOS-specific monoclonal antibody	Nakamura et al., 2006	Clone number: i2G4
Chemicals, Peptides, and Recombinant Proteins		
NAC	Wako Pure Chemical Industries	013-05133; CAS: 616-91-1
NaHS	Wako Pure Chemical Industries	517-30351; CAS: 16721-80-5
$NaNO_2$	Wako Pure Chemical Industries	197-02561; CAS: 7632-00-0
Zymosan A	Wako Pure Chemical Industries	263-01491;CAS: 58856-93-2
LPS (*Escherichia coli* 055:B5)	Sigma-Aldrich	L2880
GSH	Sigma-Aldrich	G4251; CAS: 70-18-8
GSSG	Sigma-Aldrich	G4376; CAS: 27025-41-8
IFN-β	R&D Systems	8234-MB-010
Poly I:C	R&D Systems	4287; CAS: 24939-03-5
L-Cysteine	Nacalai Tesque	10309-12; CAS: 52-90-4
HPE-IAM	Molecular BioSciences	24600; CAS: 53527-07-4
$Na_2{}^{34}S$	Wintner et al., 2010	N/A
$[^{13}C_2, ^{15}N]$GSH	Sigma-Aldrich	683620
Experimental Models: Cell Lines		
RAW264.7 cells (male)	RIKEN BioResource Center	RCB0535
Experimental Models: Organisms/Strains		
C57BL/6 Mice (male, 9-week-old)	Japan SLC Inc.	N/A
Oligonucleotides		
Primer: mouse IFN-β forward: 5'-AAACAATTTCTCCAGCACTG-3'	Sugiyama et al., 2004	N/A
Primer: mouse IFN-β reverse: 5'-ATTCTGAGGCATCAACTGAC-3'	Sugiyama et al., 2004	N/A
Primer: mouse GAPDH forward: 5'- TGAGGCCAGTGCTGAGTATG -3'	Furukawa et al., 2011	N/A
Primer: mouse GAPDH reverse: 5'- CCTTCCACAATGCCAAAGTT-3'	Furukawa et al., 2011	N/A
Software		
GraphPad Prism 7.0	GraphPad Software, La Jolla, CA, USA	www.graphpad.com

CONTACT FOR REAGENT AND RESOURCE SHARING

Further information and requests for resources and reagents should be directed to and will be fulfilled by the Lead Contact, Tomohiro Sawa (sawat@kumamoto-u.ac.jp).

EXPERIMENTAL MODEL AND SUBJECT DETAILS

Animal Models

C57BL/6 mice (male, 9-week-old) were purchased from Japan SLC Inc. (Shizuoka, Japan) and housed at the Center for Animal Resources and Development, Kumamoto University. All procedures were approved by the Kumamoto University Ethics Review Committee for Animal Experimentation (Experiment number F29-194) and were performed to minimize the number of animals used and their suffering.

Cell Lines and Culture Conditions

Cells of the murine macrophage-like cell line RAW264.7 (gender: male; RIKEN BioResource Center, Tsukuba, Japan) were cultured in Dulbecco's Modified Eagle's Medium (Wako Pure Chemical Industries, Osaka, Japan) supplemented with 10% heat-inactivated fetal bovine serum (MP Biomedicals, Santa Ana, CA, USA) and 1% penicillin-streptomycin (Nacalai Tesque, Kyoto, Japan) in a 5% CO_2 humidified incubator at 37°C.

METHOD DETAILS

Reagents

NAC, NaHS, zymosan A, and $NaNO_2$ were purchased from Wako. LPS (*Escherichia coli* 055:B5), GSH, oxidized L-glutathione (GSSG), and anti-actin antibody (A2066) were purchased from Sigma-Aldrich (St. Louis, MO, USA). L-Cysteine was purchased from Nacalai Tesque. β-(4-Hydroxyphenyl)ethyl iodoacetamide (HPE-IAM) was purchased from Molecular BioSciences (Boulder, CO, USA). Isotope-labeled sodium sulfide $Na_2{}^{34}S$ was prepared according to the literature (Wintner et al., 2010). Anti-phospho-IκBα (#9246), anti-phospho-STAT1 (#7649), anti-STAT1 (#9172), anti-phospho-NF-κB p65 (#3033), anti-phospho-ERK1/2 (#4370), anti-ERK1/2 (#4695), anti-phospho-JNK (#4668), anti-JNK (#9252), anti-phospho-Akt (#4060), anti-Akt (#4691), anti-phospho-p38 (#4511), and anti-p38 (#8690) antibodies were purchased from Cell Signaling Technology (Danvers, MA, USA). Anti-NF-κB p65 antibody (C-20, sc-372) was from Santa Cruz Biotechnology (Santa Cruz, CA, USA). Recombinant mouse IFN-β (8234-MB-010) and poly I:C (4287) were from R&D Systems (Minneapolis, MN, USA). iNOS-specific monoclonal antibody i2G4 was prepared as described previously (Nakamura et al., 2006). All reagents were of the highest grade available and used without further purification.

Preparation of NAC Polysulfides

NAC polysulfides were prepared by reacting NAC with sulfide in the presence of certain oxidants, similar to the protocol used for preparation of cysteine polysulfides as reported previously (Akaike et al., 2017; Ida et al., 2014; Ono et al., 2017). In brief, NAC (60 mM) was reacted with 60 mM $NaNO_2$ in H_2O at 37°C for 5 min, followed by addition of NaHS (final concentration, 45 mM) and formic acid (final concentration, 0.2%) and another incubation at 37°C for 15 min. The reaction mixture was subjected to preparative HPLC for purification of NAC polysulfides. Preparative HPLC was performed by using the Agilent 1260 Infinity series equipped with a photodiode array detector and an automated fraction collector (Agilent Technologies, Santa Clara, CA, USA). Samples (1500 μl) were injected onto a YMC-Triart C18 Plus column (10 × 250 mm; YMC Co., Ltd., Kyoto, Japan) at 35°C. Mobile phases A (H_2O + 0.1% formic acid) and B (acetonitrile) were used with a linear gradient from 0.2% to 40% B for 22 min, with the gradient maintained at 40% B for 1 min, after which the gradient was decreased to 0.2% B in 1 min, with a flow rate of 3 ml/min. NAC polysulfides were detected at 210 nm. Formation of NAC polysulfides was determined by means of MS as described below. Peaks corresponding to NAC polysulfides were collected by using a fraction collector and were subjected to lyophilization. NAC polysulfides labeled with ^{34}S at sulfane sulfur moieties were prepared by using $Na_2{}^{34}S$ instead of NaHS.

Preparation of HPE-AM Adduct Standards

In this study, hydropersulfides/polysulfides were quantified by means of LC-MS/MS after derivatization with HPE-IAM to form stable HPE-AM adducts (Akaike et al., 2017). For precise quantification, isotope-labeled HPE-AM adducts were spiked into samples. HPE-AM adducts of cysteine, GSH, their hydropersulfides/polysulfides, and H_2S were prepared as described previously (Akaike et al., 2017; Ida et al., 2014; Ono et al., 2017). The same protocol was applied to preparation of NAC adducts. Isotope labeling was performed by using isotope-labeled starting materials including $Cys^{34}SH$, [$^{13}C_2$,^{15}N]GSH (Sigma-Aldrich), [^{34}S]NAC, and $Na_2{}^{34}S$. $Cys^{34}SH$ and [^{34}S]NAC were synthesized by using the method reported recently (Ono et al., 2017). HPE-AM adducts of sulfite and thiosulfate were prepared by reacting 100 mM Na_2SO_3 or $Na_2S_2O_3$ with 50 mM HPE-IAM in 50 mM Tris-HCl (pH 7.4) at 37°C for 15 min. All persulfide HPE-AM adducts were purified by means of reversed-phase HPLC.

LC-MS and LC-MS/MS

NAC polysulfides, HPE-AM adducts, and related molecules were analyzed by means of LC-electrospray ionization (ESI)-MS with the Agilent 6460 Triple Quadrupole LC/MS system (Agilent Technologies). LC conditions used were as follows: column, YMC-Triart C18 Plus column (2.1 × 50 mm) (YMC Co.); column temperature, 45°C; injection volume, 1 μl; mobile phases: A, 0.1% formic acid, and B, acetonitrile; gradient (B concentration), 0 min - 1%, 10 min - 80%, 10.5 min - 1%, 15 min - 1%; flow rate, 0.2 ml/min. General conditions used for ESI-MS were as follows: nebulizer gas, nitrogen delivered at 50 psi; nebulizer gas temperature, 250°C; capillary voltage, 3500 V; collision gas, G1 grade nitrogen (Taiyo Nippon Sanso Corp., Tokyo, Japan). Multiple reaction monitoring (MRM) was used to quantify the analytes. Table S1 provides the MRM parameters used in this study.

Reaction between NAC Polysulfides and GSH

NAC polysulfides (100 μM) were reacted with GSH (10 and 100 μM) in 50 mM sodium phosphate buffer (pH 7.5) at 37°C. At various time points, 5 μl of the reaction mixtures were taken and mixed with 95 μl of 0.1% formic acid to terminate the reactions. NAC polysulfides that remained in the mixtures were quantified by means of LC-MS/MS. To identify the products formed in the reactions between NAC polysulfides and GSH, 5 mM HPE-IAM was added to the reaction mixtures containing NAC polysulfides and GSH (10 and 100 μM) after 30 min of incubation to derivatize reduced thiols. Products formed were investigated by means of LC-MS and LC-MS/MS.

Cell Treatment

RAW264.7 cells (male) were plated in 6-, 24-, or 96-well plates (at a density of 1.0×10^6 cells/well, 2.5×10^5 cells/well, and 5.0×10^4 cells/well, respectively) and allowed to grow overnight. On the day of the experiment, cells were treated with LPS (100 ng/ml), or were not treated with LPS, in the presence of NAC polysulfides, NAC, or NaHS as indicated in the figure legends. To determine the effect of NAC polysulfides on TLR2 and TLR3 signaling pathways, cells were stimulated with zymosan A (TLR2 ligand, 100 μg/ml) or poly I:C (TLR3 ligand, 25 μg/ml) in the presence of NAC polysulfides for 3 h. To examine the effect of NAC polysulfides on IFN-β-induced phosphorylation of STAT1, cells were treated with NAC polysulfides for 3 h and then stimulated with IFN-β (100 pg/ml, approximately 120 U/ml) for 10, 30, or 60 min.

Sulfur Metabolomic Analyses

We performed LC-MS/MS-based sulfur metabolomic analysis to quantify various sulfur species present in cells (Akaike et al., 2017; Ida et al., 2014; Kunikata et al., 2017; Numakura et al., 2017; Ono et al., 2017). In brief, cells treated under certain conditions were washed once with phosphate-buffered saline (PBS) and were harvested with a methanol solution containing 5 mM HPE-IAM. Cell suspensions were homogenized with a Bioruptor (Cosmo Bio, Tokyo, Japan), followed by incubation at 37°C for 15 min. After centrifugation, supernatants were diluted 10-fold with 0.1% formic acid containing known amounts of isotope-labeled standards, after which they were subjected to LC-MS/MS metabolomic analysis. Precipitates were lysed by sonication with 1% sodium dodecyl sulfate (SDS) in PBS. Protein concentrations in the precipitates were measured by using the BCA Protein Assay Kit (Wako).

Cell Viability

We determined cell viability by means of the 3-[4,5-dimethylthiazol-2-yl]-2,5-diphenyltetrazolium bromide (MTT) assay based on the mitochondrial reduction of MTT to formazan. RAW264.7 cells were seeded in a 96-well plate at a density of 5×10^4 cells/well. After overnight culture, cells were treated with LPS (100 ng/ml) and NAC polysulfides. After 3, 6, and 24 h of incubation, culture medium was replaced with 200 μl of fresh medium. A 7.5 mg/ml solution of MTT in PBS was added into each well (20 μl/well). After incubation for 1.5 h, 150 μl of culture supernatant was removed from each well and the formazan crystals were lysed by using 100 μl of MTT stop solution (0.4% HCl, 10% Triton X-100 in isopropanol). After incubation for 12 h, absorbance was measured at 570 nm, with 655 nm as the reference wavelength, via a microplate reader (Bio-Rad, Hercules, CA, USA).

Western Blotting

Cells were lysed in SDS sample buffer (62.5 mM Tris-HCl pH6.8, 2% SDS, 6% glycerol, 0.005% bromophenol blue, and 2.5% 2-mercaptoethanol) and then boiled for 5 min. Proteins were separated by using SDS-polyacrylamide gel electrophoresis and were then transferred to polyvinylidene difluoride membranes (Merck Millipore, Darmstadt, Germany) at 100 V for 1 h. Membranes were blocked with 5% non-fat milk in Tris-buffered saline (TBS) containing 0.1% Tween-20 (TBS-T) (20 mM Tris pH 7.5, 137 mM NaCl, and 0.1% Tween 20) for 60 min and then incubated for 1 h at room temperature or overnight at 4°C with the primary antibodies as indicated. After membranes were washed with TBS-T, they were incubated with horseradish peroxidase (HRP)-conjugated anti-mouse or anti-rabbit secondary antibodies (Cell Signaling Technology) at room temperature for 1 h. After samples were washed with TBS-T, protein bands were detected by using Immobilon Western Chemiluminescent HRP Substrate (Merck Millipore) with the luminescent image analyzer ChemiDoc XRS system (Bio-Rad).

Determination of Cytokine Production

Levels of the cytokines TNF-α and IFN-β in culture supernatants were measured by means of the mouse TNF-α ELISA kit (R&D Systems) and mouse IFN-β ELISA kit (PBL Assay Science, Piscataway, NJ, USA), respectively, according to the manufacturers' instructions. Absorbance at 490 nm was then measured by using an iMark Microplate Reader (Bio-Rad).

Nitrite Assay

NO production by RAW264.7 cells was determined by means of the Griess assay (Marzinzig et al., 1997). Cells were treated with LPS (100 ng/ml), or were not treated with LPS, in the presence of certain additives such as NAC polysulfides. Culture supernatants (50 μl) were collected and subjected to the Griess assay. The absorbance of samples at 570 nm was compared with that of the $NaNO_2$ standard on a microplate reader (Bio-Rad).

RT-PCR

Total RNA was extracted from RAW264.7 cells by means of the RNeasy Mini Kit (Qiagen), according to the manufacturer's protocol. Total RNA (1 μg) was reverse transcribed by using the ReverTraAce qPCR RT Kit (TOYOBO, Osaka, Japan) according to the manufacturer's instructions. cDNA was amplified by PCR by means of KOD FX polymerase (TOYOBO). The PCR conditions were as follows: initial denaturation at 94°C for 2 min, 28 cycles at 98°C for 10 s, 50°C for 30 s, and 68°C for 30 s, followed by a final step at 68°C for 5 min. Primers for PCR are given in the Key Resources Table. PCR products were subjected to electrophoresis on 2% agarose gels, and the bands were stained with ethidium bromide and visualized under UV light.

Mouse Endotoxin Shock Model

The effects of NAC polysulfides on *in vivo* inflammatory responses were studied by using the mouse endotoxin shock model (Kawai et al., 1999). Male 9-week-old C57BL/6 mice (average body weight about 25 g) received intraperitoneal injections of PBS (0.1 ml, solvent control) or LPS [20 mg/kg body weight (0.1 ml of 5 mg/ml), from *E. coli* 055:B5]. Thirty minutes later, mice received intraperitoneal injections of physiological saline (0.1 ml, solvent control), NAC polysulfides [120 μmol/kg body weight (0.1 ml of 30 mM)], or NaHS [120 μmol/kg body weight (0.1 ml of 30 mM)]. An additional treatment was performed 24 h after the first treatment. Survival of mice was monitored at 24-h intervals for 96 h after the LPS injection. Survival curves were constructed by using the Kaplan-Meier method and GraphPad Prism 7.0 (GraphPad Software, La Jolla, CA, USA). To quantify various sulfur species present in tissues, mice were killed at 27 h after the LPS injection. Livers and lungs were immediately homogenized by using the Polytron homogenizer PT1200E (Kinematica AG, Lucerne, Switzerland) in a cold methanol solution containing 5 mM HPE-IAM, followed by incubation for 20 min at 37°C. After centrifugation, aliquots of the supernatants were diluted 100-fold with 0.1% formic acid containing known amounts of isotope-labeled internal standards, which were then subjected to LC-MS/MS metabolomic analysis as described above. Precipitates were lysed by sonication with 1% SDS in PBS. Protein concentrations in the precipitates were measured by using the BCA Protein Assay Kit (Wako). Blood samples were collected from each group of mice and serum samples were obtained by centrifugation. The levels of TNF-α and IFN-β in serum samples were determined by means of the mouse TNF-α and IFN-β ELISA kits (R&D Systems) according to the manufacturer's instructions as described above.

QUANTIFICATION AND STATISTICAL ANALYSIS

All data are expressed as means ± SD. Data for each experiment were acquired from at least three independent experiments. Statistical analyses were performed by using Student's t test, with significance set at $p < 0.05$. Survival curves constructed by using the Kaplan-Meier method were analyzed by means of the log-rank (Mantel-Cox) test, with significance set at $p < 0.05$.